Methamphetamine enhances HIV-induced aberrant proliferation of neural progenitor cells via the FOXO3-mediated mechanism

Minseon Park
University of Miami Miller School of Medicine: University of Miami School of Medicine
William Baker
University of Miami Miller School of Medicine: University of Miami School of Medicine
Dilraj Cambow
University of Miami Miller School of Medicine: University of Miami School of Medicine
Danielle Gogerty
University of Miami Miller School of Medicine: University of Miami School of Medicine
Ana Rachel Leda
University of Miami Miller School of Medicine: University of Miami School of Medicine
Bridget Herlihy
University of Miami Miller School of Medicine: University of Miami School of Medicine
Darya Pavlenko
University of Miami Miller School of Medicine: University of Miami School of Medicine
Michal Toborek (mtoborek@med.miami.edu)
University of Miami Miller School of Medicine: University of Miami School of Medicine
https://orcid.org/0000-0003-4475-2119

Research article

Keywords: drug abuse, neuroinfections, gene profile, transcriptional regulation, neural progenitor cells, proliferation, subventricular zone

Posted Date: November 18th, 2020

DOI: https://doi.org/10.21203/rs.3.rs-107347/v1

Version of Record: A version of this preprint was published at Molecular Neurobiology on May 13th, 2021. See the published version at https://doi.org/10.1007/s12035-021-02407-9.

Abstract

Background

Maintaining an intact pool of neural progenitor cells (NPCs) is crucial for generating new and functionally active neurons. As intrinsic and microenvironments tightly control developmental processes of adult neurogenesis, Methamphetamine (METH) and HIV-1-mediated impairment of the blood-brain barrier and development of neuroinflammation may induce alterations in functions of NPCs; however, the combined effects of METH and HIV-1 on the NPCs are still poorly understood.

Methods

To elucidate the possible mechanisms for the enhanced proliferation of NPCs by METH exposure and HIV infection, Male C57BL/6 mice were injected with METH with an escalating dose regimen for 6 days, followed by infusion with a chimeric HIV-NDK (EcoHIV) into the left internal carotid artery to infect brains. NPCs were isolated from the subventricular zone (SVZ) and used for RNA sequencing and differential expression analysis two weeks after infection. ReNcell VM, an immortalized human NPC line were used for in vitro exposure to METH and HIV infection

Results

Chronic exposure to METH combined with brain infection by EcoHIV enhanced the proliferation of NPCs in the SVZ in mice. This effect was long-lasting as it was preserved ex vivo in NPCs isolated from the exposed mice over several passages in the absence of additional treatments. Transcriptomic studies indicated that 27 out of the top 30 differentially expressed genes response to METH plus EcoHIV were targets of the Forkhead box O transcriptional factor (FOXO), and primarily FOXO3. Additional ex vivo studies and in vitro experiments revealed the upregulation of the CXCL12-CXCR4 axis, leading to activation of downstream pAkt and pErk, the pathways that can phosphorylate FOXO3 and force its exports from the nuclei into the cytoplasm. Indeed, nuclear expulsion of FOXO3 was demonstrated both in mice exposed to METH and infected with EcoHIV and in cell culture of human NPCs.

Conclusions

These results provide novel information that exposure to METH combined with HIV infection can induce aberrant proliferation of SVZ-derived NPCs. Upregulation of CXCL12-CXCR4-Akt-1 signaling pathway exported FOXO3 into the cytoplasm, which changed the mRNA expression of FOXO3-target genes and induced the proliferation alteration as a result.

Full Text

This preprint is available for download as a PDF.

Figures

Figure 1

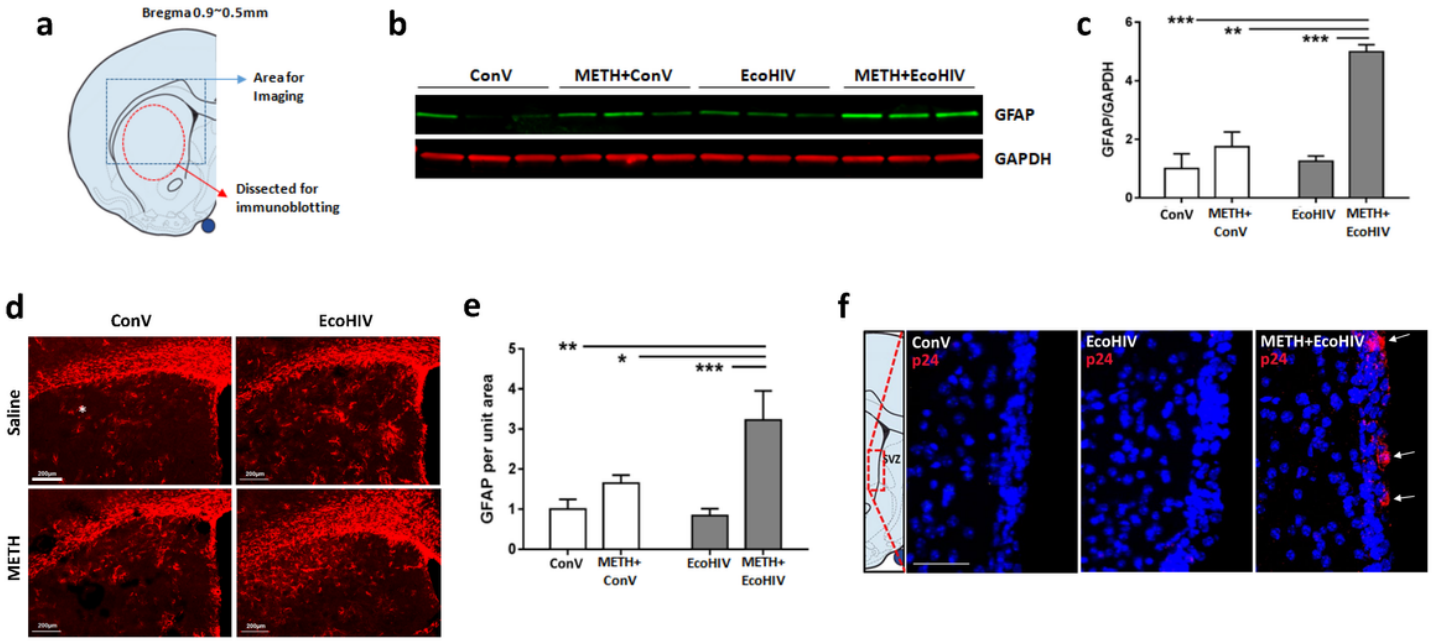

Figure 1

Validation of METH and EcoHIV neurotoxicity and neuroinflammation model. a The brain regions used for the analysis of METH and/or EcoHIV-induced neurotoxicity and neuroinflammation. Freshly collected mouse brains were cross-cut at the bregma 0.9~0.5 mm and the caudate putamen (CP) region, indicated as a dashed circle, was dissected and analyzed by immunoblotting. The dashed rectangle was the region from the frozen brain sections which was examined by immunostaining and confocal imaging. b A representative immunoblotting of GFAP in the CP region. Mice were treated with METH and/or infected with EcoHIV or control virus as described in the Methods. GAPDH was used for loading control. c Quantitative results of METH and/or EcoHIV-induced GFAP expression from (b). The intensity of the bands corresponding to GFAP was normalized to the corresponding GAPDH intensity, and the mean and SEM were calculated. N= 6 per group; two-way ANOVA; **, $p<0.01$; ***, $p<0.005$. d A representative immunostaining for GFAP. Analyses were performed on frozen brain sections visualized in (a) and imaged by confocal microscopy. Scale bar, 200 μm. e Quantitative results of GFAP immunostaining from (d). The unit intensity of each image was calculated as total fluorescence intensity divided by the total area measured. N=6 per group; two-way ANOVA; **, $p<0.01$; ***, $p<0.005$. f EcoHIV infection in the SVZ. Frozen sections of the SVZ from the treated animals were immunostained for p24 (red). Analyses were performed two weeks after EcoHIV infusion. p24 positive immunoreactivity (arrows) was detected only in METH-exposed and EcoHIV-infected brains. Scale bar, 40 μm.

Figure 2

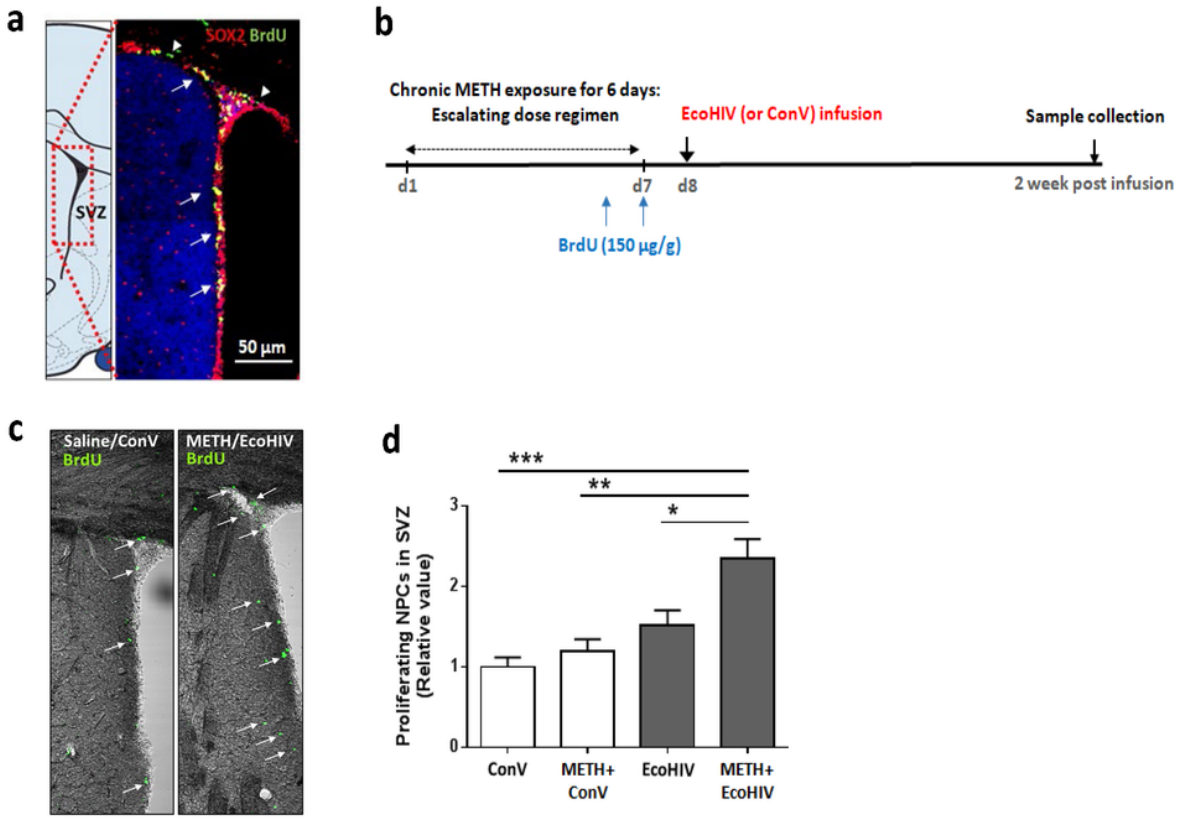

Figure 2

METH exposure and EcoHIV infection enhance NPC proliferation in the SVZ. a Visualization of proliferating NPCs in the SVZ. C57BL/6 mice were i.p. injected with BrdU (150 µg/g) once a day for two consecutive days before being sacrificed. Frozen brain sections were co-immunostained with anti-Sox2 and anti-BrdU antibodies to verify the presence of proliferating NPCs in the SVZ. Arrowheads indicate BrdU-positive cells (green) and arrows indicate Sox2 and BrdU-double positive cells (yellow). Scale bar, 50 µm. b Timeline employed in animal studies. Mice were injected i.p. with BrdU as in (a) on the last two days of METH exposure, followed by EcoHIV (or control retrovirus, ConV) infusion. Brains were collected and processed for frozen sectioning two weeks after EcoHIV infusion. c Representative images of proliferating cells in the SVZ from the control and METH plus EcoHIV brains. BrdU-positive cells (green) are identified by arrows. d Relative number of Sox 2 and BrdU-double positive cells in SVZ. Mice were exposed as in (b), then, the SVZ regions were immunostained for Sox2 and BrdU and double-positive cells were counted. N=4-5 mice per group; two-way ANOVA;*, $p<0.05$, **, $p<0.01$, and ***, $p<0.005$.

Figure 3

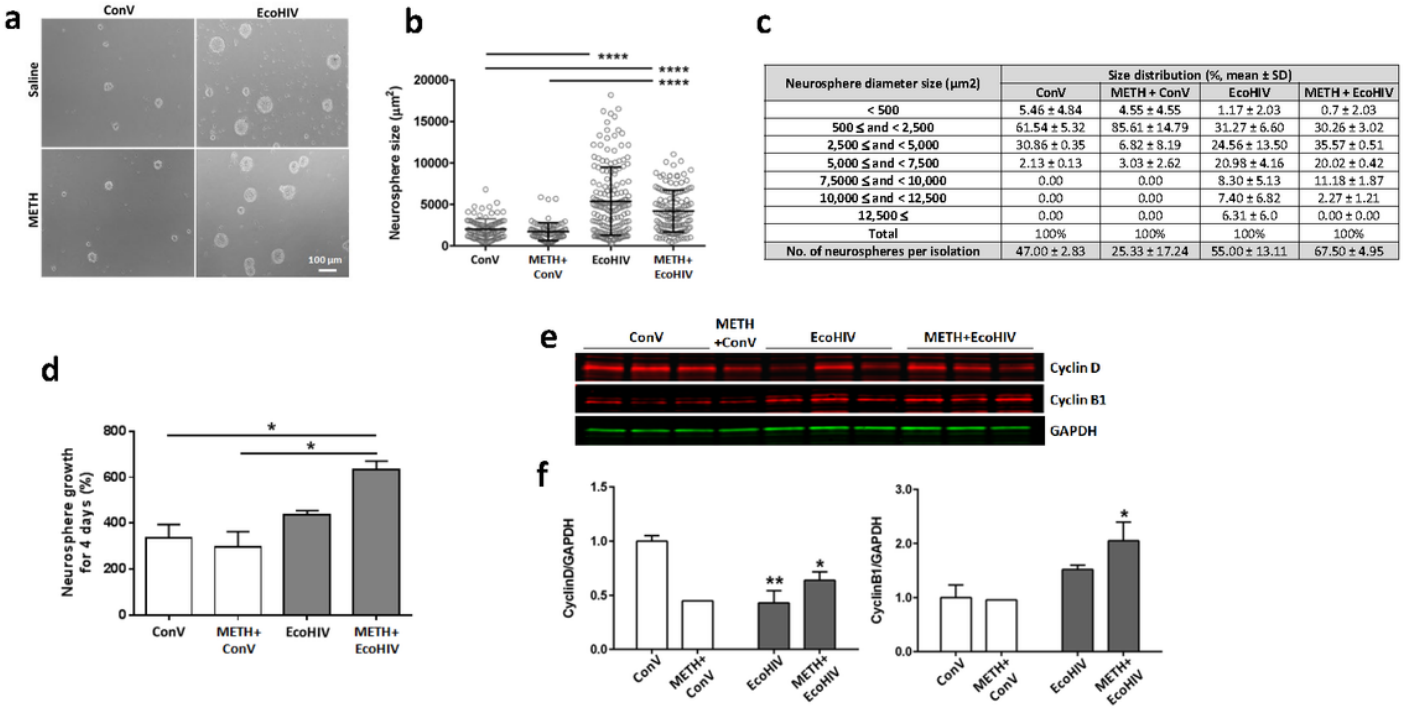

Neurosphere diameter size (µm2)	Size distribution (%, mean ± SD)			
	ConV	METH + ConV	EcoHIV	METH + EcoHIV
< 500	5.46 ± 4.84	4.55 ± 4.55	1.17 ± 2.03	0.7 ± 2.03
500 ≤ and < 2,500	61.54 ± 5.32	85.61 ± 14.79	31.27 ± 6.60	30.26 ± 3.02
2,500 ≤ and < 5,000	30.86 ± 0.35	6.82 ± 8.19	24.56 ± 13.50	35.57 ± 0.51
5,000 ≤ and < 7,500	2.13 ± 0.13	3.03 ± 2.62	20.98 ± 4.16	20.02 ± 0.42
7,5000 ≤ and < 10,000	0.00	0.00	8.30 ± 5.13	11.18 ± 1.87
10,000 ≤ and < 12,500	0.00	0.00	7.40 ± 6.82	2.27 ± 1.21
12,500 ≤	0.00	0.00	6.31 ± 6.0	0.00 ± 0.00
Total	100%	100%	100%	100%
No. of neurospheres per isolation	47.00 ± 2.83	25.33 ± 17.24	55.00 ± 13.11	67.50 ± 4.95

Figure 3

A long-term impact of METH exposure and EcoHIV infection on NPC cell cycle 592 dysregulation. a Representative images of cultured primary NPCs. SVZ-derived NPCs were isolated from freshly collected brains and cultured ex vivo. Images (phase contrast microscopy) were obtained 10 days 595 post isolation. Scale bar, 100 µm. b Quantitative measurements of neurosphere sizes from (a). Mean ± SEM; ****, p< 0.0001 vs ConV or METH+ConV. c Size distribution of isolated neurospheres from (b). Neurospheres were grouped by their sizes and the amount of neurospheres in each size range was expressed as % total. The number of neurospheres per isolation is the mean ± SEM. Two mouse brains were used per isolation as described in Methods. d Growth rate of NPCs cultured ex vivo. Single cell suspension of the third generation of NPCs was prepared and counted, and the cells were allowed to grow for 4 days to form neurospheres. The neurospheres were then dissociated and cell number was counted again. N=6 mice per group; *, p<0.05 vs ConV or METH+ConV. e Representative images of the impact of METH and/or EcoHIV on cell cycle 604 protein expression. Proteins were extracted from the seventh generation of SVZ-derived NPCs and evaluated for Cyclin B1 and Cyclin D by immunoblotting. f Quantitative results of yclin B1 and D expression from (e). The intensity of the bands corresponding to Cyclin B1 or Cyclin D was normalized to corresponding GAPDH intensity, and the mean and SEM were calculated. Two-way ANOVA, N=6 mice per group except for two mice for METH only group; *, p<0.05 and **, p<0.01 vs ConV.

Figure 4

a

DESeq2 analysis	ConV vs METH+ConV	EcoHIV vs METH+EcoHIV	ConV vs EcoHIV	METH+ConV vs METH+EcoHIV	METH by EcoHIV Interaction
Lowest P value	3.20E-04	1.91E-09	2.98E-13	2.62E-13	4.90E-08
Gene number (P<0.05)	323	837	1,756	1,537	864
Gene number (FDR<0.1)	0	28	158	229	53

b

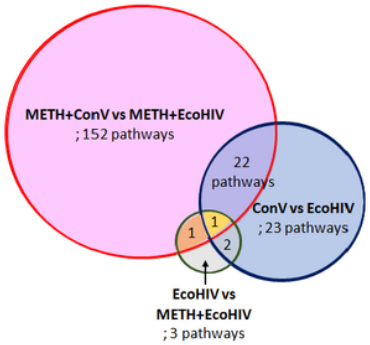

c

NPC-related pathways affected by METH+EcoHIV	Total no. of genes	Upregulated genes	Downregulated genes
Cell migration	22	11	11
Cell motility	22	11	11
Cell proliferation	26	15	11
Cell-cell signaling	24	11	13
Negative regulation of cell proliferation	13	7	6
Neuron development	18	12	6
Neuron differentiation	21	14	7
Neuron projection	15	11	4
Neuron projection development	15	11	4
Neuron projection extension	6	4	2
Neurotransmitter receptor activity	5	2	3
Positive regulation of cell differentiation	17	13	4
Positive regulation of cell proliferation	16	11	5
Regulation of cell migration	14	7	7
Regulation of extent of cell growth	5	3	2
Regulation of neuron differentiation	12	10	2

Figure 4

METH exposure and EcoHIV infection induce long term mRNA expression changes in the SVZ-derived NPCs. a Summary of the DESeq2 differential expression analysis performed on SVZ-derived NPCs of the seventh generation. b The number of functional pathways differentially affected between each pair of the treatment groups. c Selected pathways differentially expressed by the METH plus EcoHIV treatment compared to the METH-treated group.

Figure 5

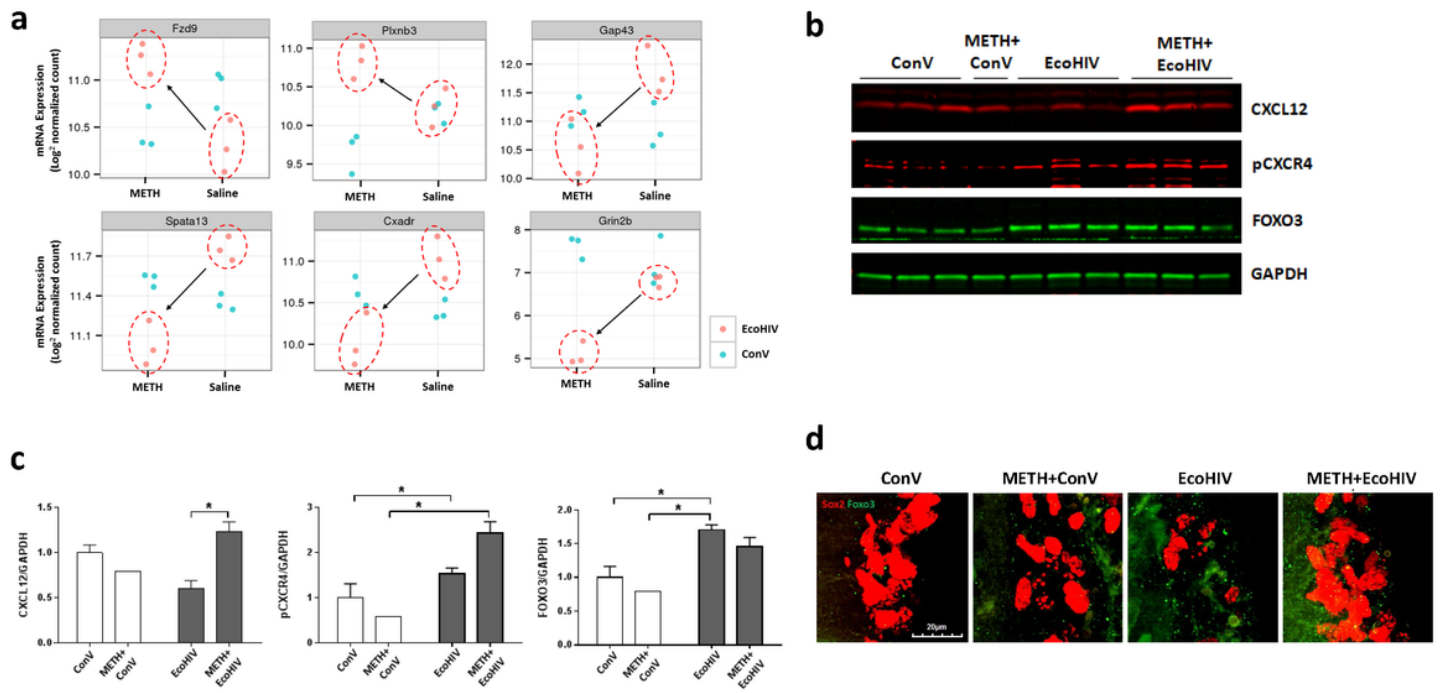

Figure 5

METH exposure and EcoHIV infection affect the expression of the CXCL12-CXCR4-FOXO3 axis. a Differentially expressed mRNAs of representative FOXO-targeted genes by METH exposure and/or EcoHIV infection in NPCs from Fig. 4. The upper plots are representative genes regulated by the FOXO family of transcription factors and the lower panels are representative FOXO3-regulated genes. b Representative immunoblots of CXCL12, phosphorylated CXCR4 (pCXCR4) and FOXO3. GAPDH was used as a loading control. c Quantitative results from (b). The intensity of the bands corresponding to CXCL12, pCXCR4, and FOXO was normalized to the orresponding GAPDH intensity, and the mean and SEM were calculated. Two-way ANOVA was used for statistical analysis. N=4-6 per group. *, $p<0.05$ and **, $p<0.01$. d Representative images 628 of FOXO3 and Sox2-positive cells in the SVZ. Mice were exposed to METH and/or infected with EcoHIV as in Fig. 2b. Frozen brain sections were immunostained for FOXO3 (green foci) and Sox2 (red) and examined under the confocal microscope. Scale bar = 20 μm; z-stacked images.

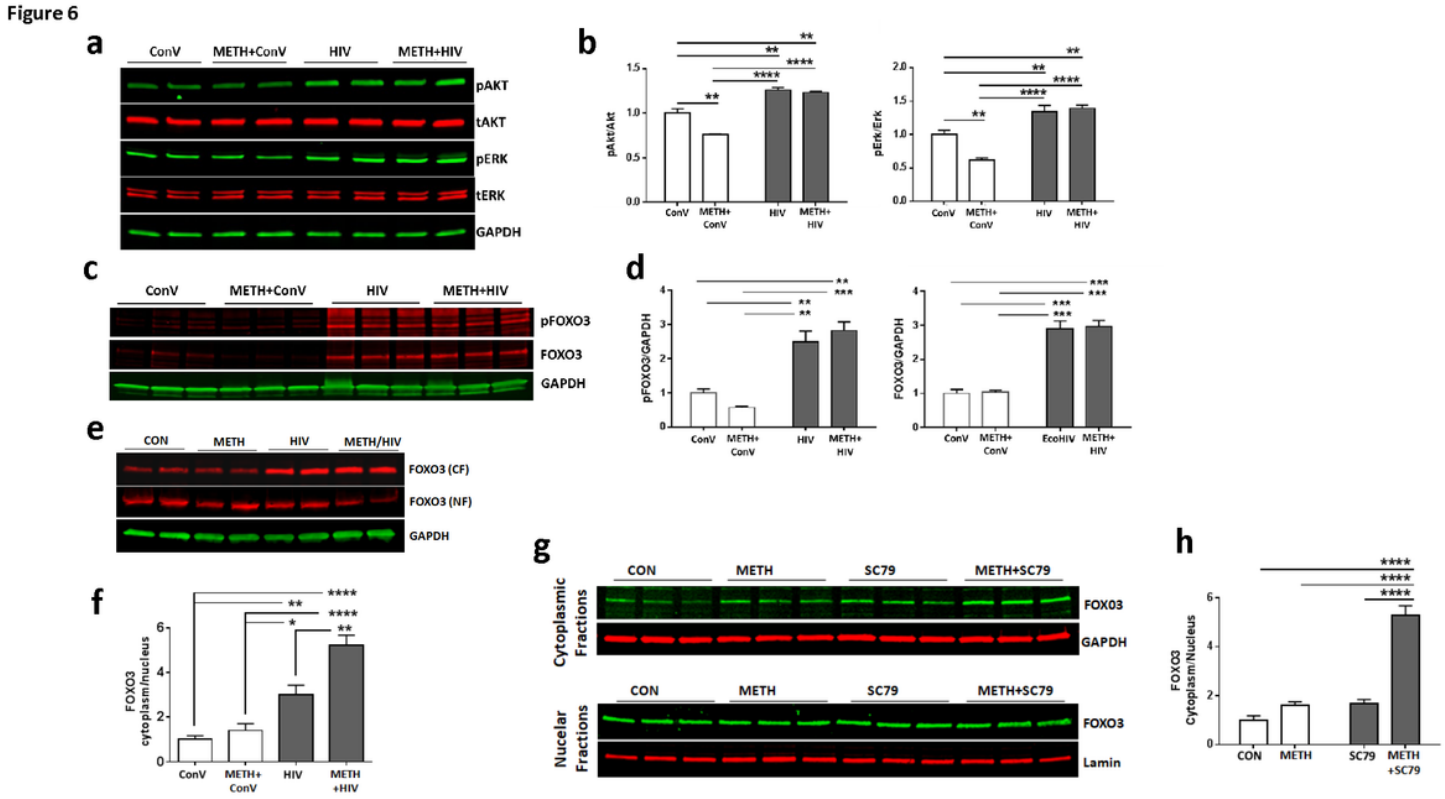

Figure 6

METH exposure and HIV infection enhance the sequestration of FOXO3 in the cytoplasm. a METH exposure and/or HIV infection-induced activation of Akt and Erk. ReNcells were 635 exposed to 100 μM METH for 24 h, followed by infection with HIV (60 ng/ml of p24) for 48 h. Cell lysates were separated on SDS-PAGE to evaluate the expression of phosphorylated and total Akt (pAkt and tAkt, respectively) as well as phosphorylated and total Erk (pErk and tErk, respectively). Representative images are presented. GAPDH was used as a loading control. b Quantitative results from (a). Two-way ANOVA, N=6 per group. **, p<0.01, and ****, p<0.001. c METH exposure and/or HIV infection-induced protein levels of phosphorylated FOXO3 (pFOXO3) and total FOXO3. Representative immunoblots. d Quantitative results from c. Two-642 way ANOVA, N=3 per group. **, p<0.01, and ***, p<0.001. e Representative images of FOXO3 in the cytoplasmic (CF) and nuclear (NF) fractions. FOXO3 protein levels were normalized to the GAPDH levels. f The ratio of FOXO3 in the cytoplasmic to nuclear fractions from €. N=6 per group. *, p<0.05, **, p<0.01, and ****, P<0.001. g Effect of Akt activator SC79 on FOXO3 subcellular localization. ReNcells were exposed to 100 μM of METH for 24 h and twice treated with 5 μM SC79 in a 24h interval. Cells were harvested 24h after the second treatment with SC79 and separated into the cytoplasmic and nuclear fractions. GAPDH and Lamin A were used as loading controls for the cytoplasmic and nuclear fractions, respectively. h The ratio of FOXO3 in the cytoplasmic to nuclear fractions from (g). N=6 per group. ****, P<0.0001.